Commun. Korean Math. Soc. **20** (2005), No. 3, pp. 589–602

A NUMERICAL ALGORITHM FOR ELASTO-PLASTIC MATERIAL DEFORMATION

HYUN-CHEOL HWANG

ABSTRACT. We present the numerical algorithm for the model for high-strain rate deformation in hyperelastic-viscoplastic materials based on a fully conservative Eulerian formulation by Plohr and Sharp. We use a hyperelastic equation of state and the modified Steinberg and Lund's rate dependent plasticity model for plasticity. A two-dimensional approximate Riemann solver is constructed in an unsplit manner to resolve the complex wave structure and combined with the second order TVD flux. Numerical results are also presented.

1. Introduction

The numerical modelling of large deformation elasto-plastic materials is challenging because the phenomena is highly nonlinear, leading to complicated wave patterns and even to material fracture or failure. The deformation gradient fields can also be discontinuous if shock waves, slip lines or material interfaces are involved. The treatment of multi-dimension problems is more difficult still. The geometry of the problem can be complex and the characteristic structure of the equations of motion is more difficult to analyze than is the case for one-dimensional problems.

Most numerical methods for such computations are Lagrangian, and are nonconservative through the use of stress variables to represent deformation states. Although the Lagrangian formulation is simpler and faster in computation since there are no convective terms for the motion of material, it suffers from severe mesh distortions, especially for problems having large deformation. Irregular Lagrangian meshes and their frequent remeshing also degrade shock propagation and cause numerical

Received December 20, 2004.

2000 Mathematics Subject Classification: 74C20, 74S10, 35L65.

Key words and phrases: elastoplasticity, viscoplasticity, conservation laws, material deformation.

diffusion. The Eulerian formulation can avoid these problems by the use of a fixed spatial grid. Also, the conservative form of the equations makes it possible to use improved numerical methods, such as a high-order Godunov or TVD method. Fully conservative Godunov methods for elastic deformation have been studied by several authors ([1, 4]), and a significant improvement resulting from the conservative formulation was reported ([1]).

In this paper, we present a numerical algorithm for modeling a two-dimensional hyperelastic-plastic solid undergoing high strain-rate deformation. Our method is an unsplit total variation diminishing (TVD) method which is second-order accurate in smooth regions and first order-accurate where shock waves or large gradients are encountered. To resolve the complex wave structure in an unsplit manner, an unsplit two-dimensional approximate Riemann solver is designed.

The content of paper is summarized as follows. In the next section, we briefly describe the conservative Eulerian formulation as our governing equations for the model of elasto-plastic materials. In section 3, we explain the details of our numerical method. The algorithm for the two-dimensional approximate Riemann solver and the TVD flux construction are explained there. In section 4, some numerical examples are illustrated and then we conclude this paper in section 5.

2. Conservative Eulerian formulation

In the conservative Eulerian formulation ([9]), the state of a deformed material body is characterized by the inverse deformation gradient, the particle velocity, a single thermodynamic variable, and several internal variables that account for plasticity. The motion of the body is determined by conservation principles.

Consider the finite deformation of a body, first from the Lagrangian point of view. Let X^α, $\alpha = 1, 2, 3$ denote the material coordinates for the (undeformed) Lagrangian configuration, and let x^i, $i = 1, 2, 3$ denote the spatial coordinates for the (current, deformed) Eulerian configuration. The motion of the material is specified by a time-dependent map ϕ^i specifying the Eulerian coordinates x^i of each material point X^α:

$$x^i = \phi^i(X^\alpha, t). \tag{2.1}$$

The gradient of ϕ^i is the matrix $F^i{}_\alpha := \partial\phi^i/\partial X^\alpha$, which is called the deformation gradient, and the time derivative of ϕ^i (with X^α fixed) is the particle velocity $V^i := \dot{\phi}^i$. Equating mixed partial derivatives yields

the conservation law $\dot{F}^i{}_\alpha = \partial V^i/\partial X^\alpha$, which represents the continuity of the body.

The corresponding Eulerian equations are based upon the inverse of the relationship (2.1):

$$X^\alpha = \psi^\alpha(x^i, t). \tag{2.2}$$

The gradient of ψ^α, denoted $g^\alpha{}_i := \partial\psi^\alpha/\partial x^i$, is called the inverse deformation gradient because when x^j and X^β are corresponding points, $g^\alpha{}_i(x^j, t)$ is the matrix inverse of $F^i{}_\alpha(X^\beta, t)$. Taking the time derivative of the identity $X^\alpha = \psi^\alpha(\phi^i(X^\beta, t), t)$, we find that the time derivative of ψ^α is $\partial\psi^\alpha/\partial t = -g^\alpha{}_k v^k$, where $v^i(x^j, t) := V^i(X^\beta, t)$ when x^j and X^β are corresponding points. Again equating mixed partial derivatives ([15]) yields the conservation law

$$\frac{\partial g^\alpha{}_i}{\partial t} + \frac{\partial\left(g^\alpha{}_j v^j\right)}{\partial x^i} = 0. \tag{2.3}$$

If $g^\alpha{}_i$ and v^i solve this equation, and if, at $t = 0$, $g^\alpha{}_i$ is the gradient of a map ψ_0^α, then there exists an inverse motion ψ^α, equaling ψ_0^α at $t = 0$, from which $g^\alpha{}_i$ and v^i derive for $t \geq 0$. Therefore, by including (2.3) among the conservation laws, we can regard $g^\alpha{}_i$ and v^i as fundamental dynamical variables, instead of ψ^α, and thereby reduce to a first-order system. See [8, 16] for further discussion.

2.1. Governing equations

The dynamics of the body is governed by the conservation law (2.3) along with conservation of momentum, conservation of energy, and the evolution equations for the internal variables.

$$\frac{\partial}{\partial t}\left(g^\alpha{}_i\right) + \frac{\partial}{\partial x^i}\left(g^\alpha{}_k v^k\right) = 0, \tag{2.4}$$

$$\frac{\partial}{\partial t}\left(\rho v^i\right) + \frac{\partial}{\partial x^j}\left(\rho v^i v^j - \sigma^{ij}\right) = 0, \tag{2.5}$$

$$\frac{\partial}{\partial t}\left(\rho e\right) + \frac{\partial}{\partial x^j}\left(\rho e v^j - \sigma^{ij} v_i\right) = 0, \tag{2.6}$$

$$\frac{\partial}{\partial t}\left(\rho E^{\mathrm{p}}_{\alpha\beta}\right) + \frac{\partial}{\partial x^k}\left(\rho E^{\mathrm{p}}_{\alpha\beta} v^k\right) = \rho\Lambda_{\alpha\beta}, \tag{2.7}$$

$$\frac{\partial}{\partial t}\left(\rho\kappa\right) + \frac{\partial}{\partial x^k}\left(\rho\kappa v^k\right) = \rho h. \tag{2.8}$$

In these equations σ^{ij} is the Cauchy stress, $e := \frac{1}{2} v_i v^i + \varepsilon$ is the total energy per unit mass, $\Lambda_{\alpha\beta}$ is the plastic source term, and h is the hardening source term.

2.2. Constitutive equations

To complete the governing system, we require constitutive equations for σ^{ij} and ε and a plastic flow rule that defines $\Lambda_{\alpha\beta}$ and h. Since we assume that the response of the material to deformation is hyperelastic, an equation of state for ε also determines σ^{ij}.

We employ a model for the specific internal energy ε founded on the assumption that the elastic shear strain ϵ remains small:

$$\varepsilon := \varepsilon_{\text{hydro}}(\tau,\eta) + \tau G(\tau,\eta)\,\epsilon^2 + O(\epsilon^3). \tag{2.9}$$

In making this choice we have combined ideas from several authors [2, 3, 10, 11, 17]. The first term represents the hydrostatic contribution to the energy and allows for large volumetric changes; the second term, in which G is the shear modulus, accounts for small elastic shear strain. For this internal energy, the Cauchy stress σ^{ij} can be calculated to be

$$\sigma^{ij} := \rho F^i{}_\alpha \frac{\partial \varepsilon}{\partial E_{\alpha\beta}} F^j{}_\beta = -p\,\delta^{ij} + G\,(\text{dev}\bar{b}_{\text{e}})^{ij} + O(\epsilon^2), \tag{2.10}$$

where $p := -\partial\varepsilon_{\text{hydro}}/\partial\tau$ is the hydrostatic pressure. (We use the notation dev$A$ for the deviator of a 3×3 matrix A, defined by dev$A := A - \frac{1}{3}(\text{tr}A)\,I$.) In the implementation of the numerical code, we neglect the higher-order terms in (2.9) and (2.10).

For $\varepsilon_{\text{hydro}}$ we use a stiffened polytropic equation of state (see [6]):

$$\varepsilon_{\text{hydro}}(\tau,\eta) := \frac{(p_0+p_\infty)}{\Gamma\rho_0}(\rho_0\tau)^{-\Gamma}\exp[\Gamma\eta/R] + p_\infty\tau, \tag{2.11}$$

where p_0, p_∞, Γ, and R are material constants. The shear modulus G is taken from the work of Steinberg et al.[12]:

$$G(\tau,\eta) := G_0\left[1 + G_p(\rho_0\tau)^{1/3}p + G_T(T-T_0)\right], \tag{2.12}$$

where G_0, G_p, and G_T are also material constants. Here the hydrostatic pressure p and temperature T are calculated as first derivatives of the hydrostatic part of the internal energy:

$$p(\tau,\eta) := -\frac{\partial\varepsilon_{\text{hydro}}}{\partial\tau}(\tau,\eta) = (p_0+p_\infty)\,(\rho_0\tau)^{-(\Gamma+1)}\exp[\Gamma\eta/R] - p_\infty, \tag{2.13}$$

$$T(\tau,\eta) := \frac{\partial\varepsilon_{\text{hydro}}}{\partial\eta}(\tau,\eta) = T_0\,(\rho_0\tau)^{-\Gamma}\exp[\Gamma\eta/R], \tag{2.14}$$

where $T_0 := (p_0+p_\infty)/(\rho_0 R)$.

For more details about the formulation such as plasticity model and flow rule, see [7, 9, 18].

3. The finite difference scheme

Equations (2.4)–(2.8) define a system of conservation laws with source terms:

$$W_t + F(W)_x + G(W)_y = H(W), \tag{3.1}$$

where $W = (\rho u, \rho v, \rho E, g_{11}, g_{12}, g_{21}, g_{22}, \rho e^p_{11}, \rho e^p_{22}, \rho e^p_{12}, \rho\kappa)^T$.

Other state variables, such as ρ, the velocities u and v, the Cauchy stress tensor Σ, the plastic strain rate λ, and the parameter Λ, are determined uniquely as long as W is given.

The method we have developed to solve (3.1) is a second order TVD finite difference scheme. Since a TVD scheme is only first-order accurate at extreme points and discontinuities, the scheme cannot be globally second-order accurate. However, we can design a scheme that is second-order accurate in smooth regions but forced to be first-order accurate near discontinuities. There are two main approaches: the slope-limiter method and the flux-limiter method. Our approach to the construction of TVD scheme can be regarded as a flux limiter method. We reconstruct the numerical flux through an integral average of Riemann solutions from neighboring meshes at the half time step. Recall that if we take the value of the Riemann solution at the t axis as an average, the result is just the first-order Godunov method. We take the average of W at the half time step,

$$W^{n+1/2}_{j+1/2} = \frac{1}{\Delta x}\int_{-\Delta x/2}^{\Delta x/2} W(\xi)\, dx, \tag{3.2}$$

for example, in the one-dimensional case. Then the scheme

$$W^{n+1}_j = W^n_j - \frac{\Delta t}{\Delta x}\left[F(W^{n+1/2}_{j+1/2}) - F(W^{n+1/2}_{j-1/2})\right] \tag{3.3}$$

is second-order accurate. If the Riemann solution, with initial data W^n_j and W^n_{j+1}, consists of N shock waves with intermediate states $W^{(k)}_{j+1/2}$ and associated wave speeds λ_k, $(k = 1, \ldots, N)$, then this average can be evaluated as

$$W^{n+1/2}_{j+1/2} = \frac{\Delta t}{2\Delta x}\Sigma_{k=1}^{N+1}(\lambda_k - \lambda_{k-1})W^{(k)}_{j+1/2}, \tag{3.4}$$

$$= \frac{1}{2}\Sigma_{k=1}^{N+1}(\nu_k - \nu_{k-1})W^{(k)}_{j+1/2}. \tag{3.5}$$

Here ν_k is a Courant number defined as $\lambda_k \frac{\Delta t}{\Delta x}$, with $\nu_0 = -1$ and $\nu_{N+1} = 1$. If W is continuous in this interval, (3.2) becomes

$$W_{j+1/2}^{n+1/2} = \frac{1}{2}(W_j + W_{j+1}) - \frac{\Delta t}{2\Delta x} \int_{W_j^n}^{W_{j+1}^n} \xi \, dW \tag{3.6}$$

after integration by parts. Here $\xi = x/t$ and $-\Delta x/2 < x < \Delta x/2$. Notice that, since $F'(W)W' = \xi W'$ when W is continuous, (3.3) is a just the two-step Lax-Wendroff method, which is the second order accurate. In other words, we can construct a scheme by combining two schemes through the proper averaging of Riemann solutions. We expand this idea to the two-dimensional case in an unsplit manner. To update all local wave interactions, we thus use an approximate, but fully two-dimensional, Riemann solver.

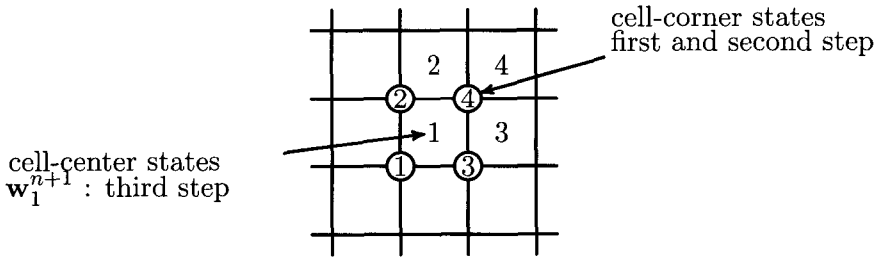

FIGURE 1. A sketch of cells and grids for constructing the numerical scheme.

Our method consists of three main steps. As in Fig 3.1, we have two different sets of state vectors in a computational domain: a cell-center valued and a cell-edge valued state. Let us assume that states at the beginning of each time step are given as cell-centered states. The first step is to find states at all edges at the half time step $t^{n+1/2}$. These are obtained by solving a two-dimensional Riemann problem approximately. The detailed algorithm for the two-dimensional approximate Riemann solver is described in the section 3.1. The next step is the construction of the TVD flux at the edge of each cell. This construction will be described in detail in section 3.2. In the third step, states at the full time step t^{n+1} at cell-centers, e.g., W_1^{n+1} in Fig 3.1, are updated implicitly by the

following unsplit scheme

(3.7)

$$
\begin{aligned}
W_1^{n+1} = W_1^n
&+ \frac{\Delta t}{2\Delta x}\left[F(W_4^{n+1/2}) + F(W_3^{n+1/2}) - F(W_2^{n+1/2}) - F(W_1^{n+1/2})\right] \\
&+ \frac{\Delta t}{2\Delta y}\left[G(W_4^{n+1/2}) - G(W_3^{n+1/2}) + G(W_2^{n+1/2}) - G(W_1^{n+1/2})\right] \\
&+ \frac{\Delta t}{8}\Big[4\,H(W_1^{n+1}) + H(W_1^{n+1/2}) + H(W_2^{n+1/2}) + H(W_3^{n+1/2}) \\
&+ H(W_4^{n+1/2})\Big],
\end{aligned}
$$

where $W_i\,(i = 1, \ldots, 4)$ are TVD states obtained in the second step. An implicit scheme is used for the stable treatment of the source term and solved iteratively, and the numerical stability is controlled by a CFL condition such as

$$CFL = \frac{c_{\max}\Delta t}{\Delta x} \leq 1. \tag{3.8}$$

Here $c_{\max} = \max|c_{\mathrm{L}} \pm u \pm v|$ is the fastest Eulerian wave speed in the entire computational domain, and c_{L} is a longitudinal wave speed which will be discussed below.

3.1. The two-dimensional approximate Riemann solver

The two-dimensional Riemann solver is an essential part of our unsplit scheme. In general, it is extremely difficult to find the exact solution of the Riemann problem even in the one-dimensional case. However, for Godunov methods, since the exact solution is expensive and is eventually averaged over each grid cell in computation, approximate Riemann solvers are widely used and are known to give equally good numerical results. In our case, we have built a two-dimensional approximate Riemann solver based on a bicharacteristic analysis of the linearized governing equations in Lagrangian coordinates. Since the convection terms are disappeared in the Lagrangian frame, the computation is faster and simpler. We find Riemann solutions in Lagrangian coordinate and then transform the solution to the Eulerian frame. This analysis also provides the characteristic wave speed information which will be used for the time step determination.

Let

$$\dot{(\,)} = \frac{\partial(\,)}{\partial t} + u\frac{\partial(\,)}{\partial x} + v\frac{\partial(\,)}{\partial y} \tag{3.9}$$

denote a Lagrangian derivative. The governing equations are transformed to the Lagrangian frame, become

$$\rho\dot{u} = \frac{\partial p}{\partial x} + \frac{\partial \tau}{\partial y},$$

$$\rho\dot{v} = \frac{\partial \tau}{\partial x} + \frac{\partial q}{\partial y}, \tag{3.10}$$

$$\rho\dot{E} = \frac{\partial}{\partial x}(pu + \tau v) + \frac{\partial}{\partial y}(\tau u + qv), \tag{3.11}$$

$$\dot{G} = -G\Omega, \tag{3.12}$$

$$\dot{E}_p = \Lambda, \tag{3.13}$$

$$\dot{\kappa} = h, \tag{3.14}$$

where Ω is the velocity gradient. Then it is possible to find all characteristic speeds by transforming the above system into following matrix form:

$$\bar{U} = A\,U_x + B\,U_y + \hat{U}, \tag{3.15}$$

and then solving

$$\det(c\,I + \cos\theta\,A + \sin\theta\,B) = 0, \quad \text{for} \quad c. \tag{3.16}$$

However, since this calculation is computationally very expensive, we need to find proper approximation. In the case of elastic-plastic materials, there are always two wave modes: longitutional and transverse waves constructing two Monge cones, the c_{L}-cone and the c_{T}-cone, at the intersection points of four quadrants. These cones represent the propagating wave front of the longitutional wave and transverse wave, respectively. This method simplifies the computation of the complex wave structure. The domain between the c_{L}-cone and the c_{T}-cone is decomposed into four regions and assumed to be a constant state within each region. Then, our two-dimensional approximate Riemann solver should return four intermediate states between the c_{L}-cone and the c_{T}-cone, i.e., W_1^i, W_2^i, W_3^i, and W_4^i, as well as states lying outside the c_{L}-cone, in addition to a state W' lying inside the c_{T}-cone. (See Fig 2.)

First, we need to find the Lagrangian wave speed c_{L} and c_{T}. In general, the wave speed is expressed as the isotropic linear wave speed plus

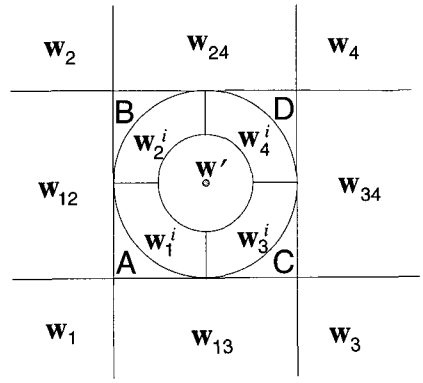

FIGURE 2. Subdomains in the Lagrangian frame to define the solution for the two-dimensional Riemann problem.

some correction term, i.e.,

$$
\begin{aligned}
c_{\mathrm{L}}^2 &= c_{\mathrm{K}}^2 + 4\mu/(3\rho) + \delta_{\mathrm{L}}, \\
c_{\mathrm{T}}^2 &= \mu/\rho + \delta_{\mathrm{T}},
\end{aligned}
\tag{3.17}
$$

where c_{K} is the bulk wave speed, and δ_{L} and δ_{T} represent corrections of order $\bar{\epsilon}$ dependent on the angle of propagation. In usual metallic materials, the order $\bar{\epsilon}$ terms are very small, so the terms δ_{L} and δ_{T} are neglected. The bulk wave speed is calculated as a derivative of mean pressure with respect to mass density at constant $\bar{\epsilon}^2$ and entropy η,

$$
c_{\mathrm{K}}^2 = \frac{\partial}{\partial \rho}\left[\mathcal{P} + \rho^2 \bar{\epsilon}^2 \frac{\partial}{\partial \rho}\left(\frac{\mu(\rho,\eta)}{\rho}\right)\right]_{\bar{\epsilon}^2,\eta}.
\tag{3.18}
$$

Therefore, the two wave speeds are computed approximately as

$$
c_{\mathrm{T}} = \sqrt{\frac{\mu(\rho,\eta)}{\rho}}, \quad c_{\mathrm{L}} = \sqrt{c_{\mathrm{K}}^2 + \frac{4}{3}c_{\mathrm{T}}^2}.
\tag{3.19}
$$

The next step is to find all states in the different regions. Let us find W' which lies inside the c_{T}-cone first. This state is obtained by integrating (3.10)–(3.14) across two Monge cones. The velocities u and

v at point P are calculated as follows:

$$
\begin{aligned}
u' &= \frac{1}{4}(u_1+u_2+u_3+u_4) \\
&\quad + \frac{1}{4\rho c_{\mathrm{L}}}(p_4+p_3-p_2-p_1) + \frac{1}{4\rho c_{\mathrm{T}}}(\tau_4-\tau_3+\tau_2-\tau_1), \\
v' &= \frac{1}{4}(v_1+v_2+v_3+v_4) \\
&\quad + \frac{1}{4\rho c_{\mathrm{T}}}(\tau_4+\tau_3-\tau_2-\tau_1) + \frac{1}{4\rho c_{\mathrm{L}}}(q_4-q_3+q_2-q_1).
\end{aligned} \tag{3.20}
$$

Here, ρc_{L} and ρc_{T} are distinct from cell to cell; however, we omit the cell indices for simplicity. In the same way, we then calculate the total energy per unit mass E and the inverse deformation matrix G. The density $\rho' = \rho_0 \det G'$ will be calculated once G' is known.

Finally, we compute the plastic strain components from (3.14) implicitly by

$$
\begin{aligned}
E'_{\mathrm{p}} &= \frac{1}{4}\left[(E_{\mathrm{p}})_1+(E_{\mathrm{p}})_2+(E_{\mathrm{p}})_3+(E_{\mathrm{p}})_4\right] \\
&\quad + \frac{\Delta t}{16}\left(4\,\Lambda(E'_p)+\Lambda_1+\Lambda_2+\Lambda_3+\Lambda_4\right),
\end{aligned} \tag{3.21}
$$

and κ is computed similarly. Thus, we have finished the computation for all state variables inside the c_{T}-cone.

Next, let us find four states, $W_1^i, \cdots, W_4^i$, lying between the c_{L}-cone and the c_{T}-cone. If one examines each term in the formula for W', it can be determined that the state inside the c_{T}-cone consists of four contributions coming from the initial state, the c_{L}-wave, the c_{T}-wave, and the source term. Therefore, the intermediate states between the c_{T}-cone and c_{L}-cone can be approximated by adding the contribution of the c_{L}-wave to the initial state. The four intermediate velocity components of u are calculated by the formula

$$
u_j^i = u_j + \frac{a_x}{\rho c_{\mathrm{L}}}(p' - p_j), \tag{3.22}
$$

where $a_x = 1$ for cells $j = 1, 2$, and $a_x = -1$ for cells $j = 3, 4$. The intermediate velocity components of v are calculated similarly. The intermediate internal energies are calculated by

$$
E_j^i = E_j + \frac{a_x}{\rho c_{\mathrm{L}}}(p'u_j^i - p_j u_j) + \frac{a_y}{\rho c_{\mathrm{L}}}(q'v_j^i - q_j v_j). \tag{3.23}
$$

For the intermediate state of G we first calculate a diagonal matrix

$$
C_j = \mathrm{diag}\left(a_x\left(u' - u_j\right)/c_{\mathrm{L}},\ a_y\left(v' - v_j\right)/c_{\mathrm{L}},\ 0\right). \tag{3.24}
$$

Then G is obtained by

$$G_j^i = G_j \left(I - \frac{1}{2}C_j\right)\left(I + \frac{1}{2}C_j\right)^{-1}. \tag{3.25}$$

There are no contributions from the c_{L}-wave and the c_{T}-wave to the plastic parameters E_{p} and κ. Therefore, we assign $(E_{\mathrm{p}})_j^i = (E_{\mathrm{p}})_j$, $\kappa_j^i = \kappa_j$ for the intermediate states.

The four states W_{12}, W_{13}, W_{24}, W_{34}, are created by a one-dimensional Riemann solution, which is a special case in the above-mentioned two-dimensional problem. The four states in the subdomains A, B, C and D are calculated by the superposition method. e.g., the state in subdomain A is calculated by

$$W_{\mathrm{A}} = W_{12} + (W_{13} - W_1). \tag{3.26}$$

Therefore, we obtain the approximate solution for all subdomains, and complete the approximate solution of the two-dimensional Riemann problem.

3.2. The higher order TVD flux construction

Higher order TVD fluxes are constructed by substituting integral averages of Riemann solutions into the original flux function. To reduce spurious oscillation near discontinuities and to maintain higher order accuracy in smooth regions, we need a good limiter dependent on the smoothness of solutions. We assume that the Riemann solution consists of N shock waves. Using a limiter ϕ_k, the TVD state from (3.6) is expressed as:

$$W_{j+1/2}^{n+1/2} = \frac{1}{2}(W_j + W_{j+1}) - \frac{1}{2}\Sigma_{k=1}^{N+1}\phi_k(W^{(k)} - W^{(k-1)}). \tag{3.27}$$

ϕ_k is the function of a local Courant number and a wave parameter ζ_k, which is defined as the ratio of the upwind change to the local change in the state variables:

$$\zeta_k = (W_j^{(k)} - W_{j-1}^{(k)})/(W_{j+1}^{(k)} - W_j^{(k)}), \tag{3.28}$$

in the case of a right-facing wave. The wave parameter expresses how rapidly the solution is changing during a computation. If $\phi_k = 1$, then the flux limited scheme is just a first-order Godunov scheme, and if ϕ_k is a local Courant number, the scheme reduces to (3.5) which is second-order accurate. In general, ϕ changes with the wave parameter ζ, and various choices of ϕ are possible [13, 14].

In our case, we use the wave information from the approximate Riemann solver and determine wave parameters and limiters which lead to a second-order TVD scheme like the linear elasticity case ([5]).

4. Numerical examples

We present some of numerical results obtained from our implementation. The example is a two dimensional Riemann problem to test our Riemann solver. Consider an infinite body domain with neither pre-stress nor initial deformation. The velocity components are all zero except in the second quadrant $x < 0$, $y > 0$ where $u = 1$ km/sec. We calculate the early state of motion and deformation in this body. The material is tantalum and material parameters are given as: $\rho_0 = 16.69$ gram/cm^3, $p_0 = 0$, $p_\infty = 51.0716$ GPa, $\gamma = 3.8$, $T_0 = 300$ K, $\mu_0 = 69$ GPa, $\mu_p = 0.0145$ 1/GPa, $\mu_t = -0.13 \cdot 10^{-3}$ 1/K, $Y_A = 0.375$ GPa, $Y_{\max} = 0.45$ GPa, $\alpha = 0.283$, $\beta = 22$, $C_1 = 0.71$ $1/\mu$s, $C_2 = 2.4$ GPa$\cdot\mu$s, $U_k/k = 3597.5$ K, $Y_P = 0.82$ GPa. The example in 3 is the case of hyperelastic material with viscoplastic effects. Here two kinds of shock waves appear: a c_{L}-wave propagating in the x-direction due to the pressure effects on the region $y > 0$, and a c_{T}-wave propagating in the y-direction due to the shear effects on the region $x < 0$. A continuous region in the fourth quadrant $x > 0$, $y < 0$ connects the two shocks. The computational results for the stress components $-p$ and τ at the time step 40 are plotted in Fig 3. The two-dimensional TVD method with the approximate Riemann solver gives second-order convergence in the continuous region, and the shocks are resolved well over about 3-5 zones. Significant decay effects from plasticity, applying both to the shock wave fronts and to the smooth regions, have appeared in the solution.

5. Conclusion

We have developed an unsplit two-dimenisional Riemann solver for the model of elasto-plastic materials and successfully apply it to higher order TVD flux. This numerical algorithm can be applied to model complex wave propagation in elasto-plastic materials, specially for the high-strain rate deformation of hyperelastic-viscoplastic materials. This Riemann solver also can be applied to front tracking method to resolve the material interface and complex shock waves appearing in impact problems.

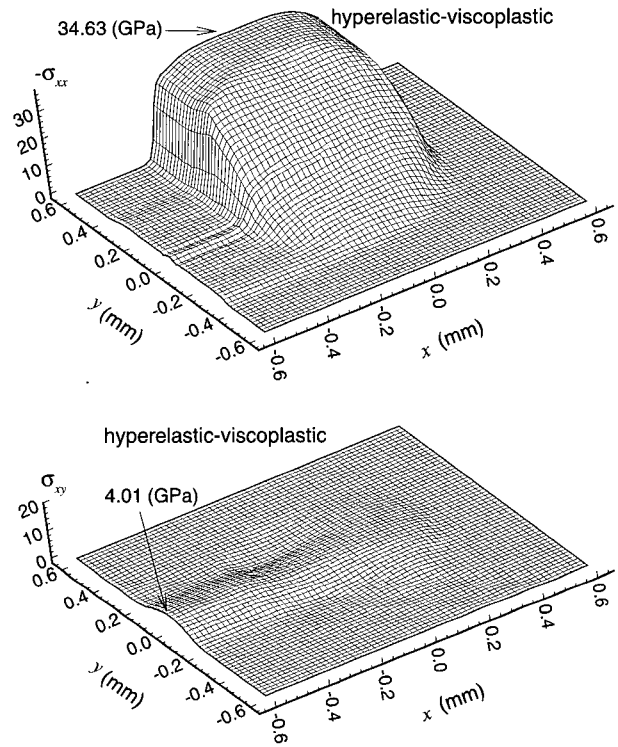

FIGURE 3. Distributions of stresses $-p = -\sigma_{xx}$ and $\tau = \sigma_{xy}$ for the two-dimensional Riemann problem for a hyperelastic-viscoplastic material, computed by two-dimensional TVD method.

ACKNOWLEDGMENTS. The author is grateful to Dr. Xiao Lin in Model Validation Team, CitiBank, U.S.A., for his encouragement and valuable advice in preparing this manuscript. This research was supported by Kyungwon University Research Fund.

References

[1] E. Bonnetier, H. Jourdren, and P. Veysseyre, *Un Modèle Hyperélastique-Plastique Eulérien Applicable aux Grandes Déformations: Quelques Résultats 1-D*, Tech. Report preprint, Centre d'Etudes de Limeil-Valenton, 1991.

[2] X. Garaizar, *The Small Anisotropy Formulation of Elastic Deformation*, Acta Appl. Math. **14** (1989), 259-268.

[3] P. Germain and E. Lee, *On Shock Waves in Elastic-Plastic Solids*, J. Mech. Phys. Solids, **21** (1973), 359–382.

[4] P. LeFloch and F. Olsson, *A second-order Godunov method for the conservation laws of nonlinear elastodynamics*, Impact Comput. Sci. Engrg. **2** (1990), 318–354.
[5] X. Lin and J. Ballmann, *A Numerical Scheme for axisymmetric elastic waves in solids*, Wave Motion **21** (1995), 115–126.
[6] R. Menikoff and B. Plohr, *The Riemann Problem for Fluid Flow of Real Materials*, Rev. Mod. Phys. **61** (1989), 75–130.
[7] B. Plohr, *Mathematical Modeling of Plasticity in Metals*, Mat. Contemp. **11** (1996), 95–120.
[8] B. Plohr and D. Sharp, *A Conservative Eulerian Formulation of the Equations for Elastic Flow*, Adv. Appl. Math. **9** (1988), 481–499.
[9] ———, *A Conservative Formulation for Plasticity*, Adv. Appl. Math. **13** (1992), 462–493.
[10] M. Scheidler, *On the Coupling of Pressure and Deviatoric Stress in Hyperelastic Materials*, Proceedings of the 13th Army Symposium on Solid Mechanics (S.-C. Chou, and F. Bartlett. T. Wright. and K. Iyer, EDS.), 1994.
[11] J. Simo and M. Ortiz, *A Unified Approach to Finite Deformation Elastoplastic Analysis Based on the Use of Hyperelastic Constitutive Relations*, Comput. Methods Appl. Mech. Engrg. **49** (1985), 221-245.
[12] D. Steinberg, S. Cochran, and M. Guinan, *A Constitutive Model for Metals Applicable at High Strain-Rate*, J. Appl. Phys. **51** (1980), 1498–1504.
[13] E. F. Toro, *The weighted average flux method applied to the Euler equations*, Phil. Trans. Royal Soc. London, **A** (1992), no. 341, 499–530.
[14] ———, *The weighted average flux method for hyperbolic conservation laws*, Phil. Trans. Royal Soc. London, **A** (1989), no. 423, 401–418.
[15] J. Trangenstein and P. Colella, *A Higher-Order Godunov Method for Modeling Finite Deformation in Elastic-Plastic Solids*, Comm. Pure Appl. Math. **XLIV** (1991), 41–100.
[16] D. Wagner, *Conservation Laws, Coordinate Transformations, and Differential Forms*, Proceedings of the Fifth International Conference on Hyperbolic Problems Theory, Numerics, and Applications (j. Glimm, M. J. Graham, J. W. Grove, and B. J. Plohr, eds.), World Scientific Publishers, Singapore, 1996, 471–477.
[17] D. Wallace, *Thermoelasticity Theory of Stressed Crystals and Higher-Order Elastic Constants*, Solid State Physics (H. Ehrenreich, F. Seitz, and D. Turnbull, eds.), Academic Press, New York **25** (1970), 301–403
[18] F. Wang, J. Glimm, J. Grove, B. Plohr, and D. Sharp, *A Conservative Eulerian Numerical Scheme for Elasto-Plasticity and Application to Plate Impact Problems*, Impact Comput. Sci. Engrg. **5** (1993), 285–308.

Department of Mathematics and Information
Kyungwon University
Songnam 461-701, Korea
E-mail: hchwang@mail.kyungwon.ac.kr